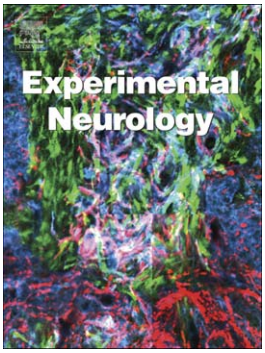

Anti-high mobility group box 1 antibody exerts neuroprotection in a rat model of Parkinson's disease

Tatsuya Sasaki, Keyue Liu, Takashi Agari, Takao Yasuhara, Jun Morimoto, Mihoko Okazaki, Hayato Takeuchi, Atsuhiko Toyoshima, Susumu Sasada, Aiko Shinko, Akihiko Kondo, Masahiro Kameda, Ikuko Miyazaki, Masato Asanuma, Cesario V. Borlongan, Masahiro Nishibori, Isao Date

PII: S0014-4886(15)30117-5
DOI: doi: 10.1016/j.expneurol.2015.11.003
Reference: YEXNR 12150

To appear in: *Experimental Neurology*

Received date: 3 August 2015
Revised date: 28 October 2015
Accepted date: 6 November 2015

Please cite this article as: Sasaki, Tatsuya, Liu, Keyue, Agari, Takashi, Yasuhara, Takao, Morimoto, Jun, Okazaki, Mihoko, Takeuchi, Hayato, Toyoshima, Atsuhiko, Sasada, Susumu, Shinko, Aiko, Kondo, Akihiko, Kameda, Masahiro, Miyazaki, Ikuko, Asanuma, Masato, Borlongan, Cesario V., Nishibori, Masahiro, Date, Isao, Anti-high mobility group box 1 antibody exerts neuroprotection in a rat model of Parkinson's disease, *Experimental Neurology* (2015), doi: 10.1016/j.expneurol.2015.11.003

Title

Anti-high mobility group box 1 antibody exerts neuroprotection in a rat model of Parkinson's disease

Author name

Tatsuya Sasaki,[1] Keyue Liu,[2] Takashi Agari,[1] Takao Yasuhara,[1] Jun Morimoto,[1] Mihoko Okazaki,[1] Hayato Takeuchi,[1] Atsuhiko Toyoshima,[1] Susumu Sasada,[1] Aiko Shinko,[1] Akihiko Kondo,[1] Masahiro Kameda,[1] Ikuko Miyazaki,[3, 4] Masato Asanuma,[3, 4] Cesario V. Borlongan,[5] Masahiro Nishibori,[2]and Isao Date[1]

Affiliation

[1]Department of Neurological Surgery, [2]Pharmacology and Pathology, [3]Brain Science, and [4]Medical Neurobiology, Okayama University Graduate School of Medicine, Dentistry and Pharmaceutical Sciences, Okayama, Japan

[5]Department of Neurosurgery and Brain Repair, University of South Florida Morsani College Medicine, Tampa, Florida, USA

Address

[1-4]Address: 2-5-1, Shikata-cho, Kita-ku, Okayama, JAPAN 700-8558

Tel: +81-86-235-7336

[5]12901 Bruce B Downs Blvd, Tampa, Florida 33612

Corresponding Author

Takao Yasuhara, MD, PhD

E-mail: tyasu37@cc.okayama-u.ac.jp

Address: 2-5-1, Shikata-cho, Kita-ku, Okayama, JAPAN 700-8558

Tel: +81-86-235-7336

Abstract

The high mobility group box-1 (HMGB1), exists as an architectural nuclear protein in the normal state, but displays an inflammatory cytokine-like activity in the extracellular space under pathological condition. Inflammation in the pathogenesis of Parkinson's disease (PD) has been documented. In this study, we investigated the involvement of HMGB1 in the pathology and the neuroprotective effects of neutralizing anti-HMGB1 monoclonal antibody (mAb) on an animal model of PD. Adult female Sprague-Dawley rats were initially injected with 6-hydroxydopmaine (6-OHDA, 20 μg / 4 μl) into the right striatum, then anti-HMGB1 mAb (1 mg/kg), or control mAb was intravenously administered immediately, at 6 and 24 hours after 6-OHDA injection. The treatment with anti-HMGB1 mAb significantly preserved dopaminergic neurons in substantia nigra pars compacta and dopaminergic teminals inherent in the striatum, and attenuated PD behavioral symptoms compared to control mAb-treated group. HMGB1 was retained in the nucleus of neurons and astrocytes by inhibiting the proinflammation-induced oxidative stress in anti-HMGB1 mAb-treated group, whereas HMGB1 translocation was observed in neurons at 1 day and astrocytes at 7 days after 6-OHDA injection in control mAb-treated group. Anti-HMGB1 mAb inhibited the activation of microglia, disruption of blood-brain-barrier (BBB), and the expression of inflammation cytokines such as IL-1β and IL-6. These results suggested that HMGB1 released from neurons and astrocytes was at least

partly involved in the mechanism and pathway of degeneration of dopaminergic neurons induced by 6-OHDA exposure. Intravenous administration of anti-HMGB1 mAb stands as a novel therapy for PD possibly acting through the suppression of neuroinflammation and the attenuation of disruption of BBB associated with the disease.

Keywords

High mobility group box 1, Parkinson's disease, neuroprotection, inflammation, antibody therapy, blood-brain-barrier

Acknowledgements

We thank Masako Arao and Natsuki Uemori for their technical assistance. This work was supported by grants from Scientific Research from the Ministry of Health, Labor, and Welfare of Japan (09156274), from the Japan Society for the Promotion of Science (JSPS Nos. 21390071, 21590594, 2365968703, 24390061), and from Natural Mutual Insurance Federation of Agricultural Cooperatives. Author contributions are the following: conceived and designed the experiments: TS KL TA TY MK AK MN ID, performed the experiments: TS KL JM MO HT AT SS AS IM, analyzed the data: TS TY CVB, contributed reagents/materials/analysis tools: TS KL IM MA MN., wrote the manuscript: TS TA TY ID CVB.

Introduction

Parkinson's disease (PD) is a typical neurodegenerative disease that is clinically characterized by muscular rigidity, resting tremor, bradykinesia and postural reflex disorder. Currently, dopamine replacement therapy using L-dopa, dopamine receptor agonists and other agents is established as a gold standard of treatment for PD. Although surgical therapy including subthalamic nucleus or globus pallidus internus stimulation is also performed for PD in advanced stage, these approaches remain palliative at best. Therefore it is necessary to develop therapeutic agents with a different mode of action from the dopamine replacement therapy. The main pathology of PD is a loss of dopamine neurons in the substantia nigra pars compacta (SNc). Despite numerous basic research investigation, the underlying pathology of PD remains not fully understood. The involvement of neuroinflammation in the pathology of PD was reported in clinical settings as well as in experimental disease models. A large number of HLA-DR positive activated microglia was detected within the SNc of PD patients at postmortem (McGeer et al., 1988). Furthermore, a surge in MHC class II (CR3/43) positive microglia was shown to infiltrate the putamen, as well as the SNc of PD patients (Imamura et al., 2003). In an animal model of PD, employing intrastriatal injection of 6-hydroxydopmaine (6-OHDA), activated microglia was identified both in the SNc and striatum (Cicchetti et al., 2002; Depino et al., 2003; He et al., 2001).

High mobility group box 1 (HMGB1) is highly conserved non-histone nuclear protein and contributes to the architecture of chromatin DNA. HMGB1 also belongs to a damage-associated-molecular-pattern (DAMP) family (Lotze and Tracey, 2005; Tsung et al., 2014) and can be passively released from damaged cell to exacerbate inflammation through the receptors including receptor for advanced glycation end products (RAGE) and toll-like receptors (TLR2 and TLR4) (Park et al., 2004; Raman et al., 2006; Yang et al., 2006). The release of HMGB1 has been reported in various diseases such as septic shock (Wang et al., 1999; Yang et al., 2004), arthritis (Hamada et al., 2008), acute myocardial infarction (Andrassy et al., 2008) and acute pancreatitis (Sawa et al., 2006; Yasuda et al., 2006). Furthermore, released HMGB1 acts as a neuroinflammatory factor in central nervous system (CNS) disease such as ischemia, traumatic brain injury and spinal nerve ligation (Kawabata et al., 2010; Kim et al., 2006; Liu et al., 2007; Okuma et al., 2012; Zhang et al., 2011). Interestingly, anti-HMGB1 monoclonal antibody (mAb) neutralized the released HMGB1, prevented the inflammation cascade, and afforded a therapeutic effect in experimental model of ischemia and traumatic brain injury (Liu et al., 2007; Okuma et al., 2012; Shichita et al., 2012; Zhang et al., 2011).

In the present study, we explored behaviorally and immunohistochemically neuroprotective effects of intravenous injection of anti-HMGB1 mAb on rat model of PD. Additionally, we examined the mechanisms of action underlying these neuroprotective effects

by investigating the inhibition of HMGB1 translocation in neurons and astrocytes, the blockade of activation of microglia, the amelioration of disruption of blood-brain-barrier (BBB) and the suppression of production of inflammatory cytokines.

Material and Methods

Animals and animal care

All experimental procedures were conducted in accordance with the Okayama University guidelines for animal experiments and were approved by the University's committee on animal experimentation. Adult female Sprague-Dawley rats, weighing 200 to 250 g, were purchased from SHIMIZU Laboratory Supplies Co., Ltd and were used for all experiments (n = 101). They were housed two per cage in a temperature- and humidity-controlled room which was maintained on a 12 h light/dark cycle with free access to food and water.

Surgical procedures

6-OHDA lesion

All rats were anesthetized with sodium pentobarbital (35 mg/kg, i.p.) and placed in a stereotaxic apparatus (Narishige, Tokyo, Japan). A midline skin incision was made and a hole was then drilled in the skull. After this procedure, 6-OHDA (20 μg, 5 mg/ml, dissolved in 0.9% saline containing 0.2 mg/ml ascorbic acid; Sigma-Aldrich, St. Louis, MO, USA) was injected

into the right striatum with a 28-gauge Hamilton Syringe (1.0 mm anterior, 2.5 mm lateral to the bregma, and 5.0 mm ventral to the surface of the brain with the tooth-bar set at -2.5 mm). The injection rate was 1 μl/min. After the injection, the syringe was left in the striatum for an additional 5 min before being retracted slowly (1 mm/min).

Administration of anti-HMGB1 mAb and appropriate controls

Anti-HMGB1 mAb (immunoglobulin, ［IgG］2a subclass, 1 mg/kg), or class-matched control mAb (IgG2a) against *Keyhole Limpet* hemocyanin (both previously described; Liu et al., 2007) was intravenously administered three times, immediately, 6 h and 24 h after 6-OHDA injection. Control mAb was confirmed to have no neuroprotective effects on a rat model of PD as preliminary investigation by assessment of motor function and tyrosine hydroxylase immunohistochemistry in the striatum and the SNc (data not shown).

Assessment of motor function

Cylinder test

The cylinder test was conducted to assess the degree of forepaw asymmetry. All rats were individually placed in a transparent cylinder (diameter: 20 cm, height: 30 cm) for 3 min and the number of forepaw contacts to the cylinder wall was counted (Schallert et al., 2000). The score of cylinder test in this study was calculated as a contralateral bias, using the following formula: [(the number of contacts with the contralateral limb) - (the number of contacts with the

ipsilateral limb)/(the number of total contacts) x100] (Roof et al., 2001; Shinko et al., 2014).

Amphetamine-induced rotation test

All rats were challenged with established drug-induced rotational test, using amphetamine (3.0 mg/kg, i.p. Dainippon Sumitomo Pharma, Japan), at 7 and 14 days after 6-OHDA injection. The rotational behaviors were assessed for 90 min with a video camera. Full 360° turns ipsilateral to the lesion were counted.

Fixation and sectioning

All rats were deeply anesthetized with sodium pentobarbital (100 mg/kg, i.p.), perfused from the ascending aorta with 200 ml of cold phosphate buffered saline (PBS), followed by 200 ml of 4% paraformaldehyde (PFA) in PBS. Brains were removed and preserved in 4% PFA.

Tyrosine hydroxylase (TH) immunohistochemical investigations

The fixed brains harvested at 14 days after 6-OHDA injection were then immersed in 30% sucrose in phosphate buffer (PB) until completely submerged and six series of coronal sections were cut at a thickness of 35 μm with a freezing microtome and stored at -20 degrees C. Free-floating sections were blocked with 3% hydrogen peroxide in 70% methanol for 8 min. Sections were washed 3 times for 5 min each time in PBS. Sections were then incubated overnight at 4 degrees C with rabbit anti-TH antibody (1:500; Chemicon, Temecula, CA, USA)

with 10% normal horse serum. After several rinses in PBS, sections were incubated for 1 hour in biotinylated donkey anti-rabbit IgG (1:500; Jackson Immuno Research Lab, West Grove, PA, USA), then for 30 min in avidin-biotin-peroxidase complex (Vector Laboratories, Burlingame, CA, USA). Subsequently, the sections were treated with 3, 4-diaminobenzidine (DAB; Vector) and hydroxygen peroxide, mounted on albumin-coated slides and embedded with cover glass.

Fluorescent immunostaining

In order to explore distribution of HMGB1 in neuron, astrocyte and microglia, immunofluorescence for double-staining of HMGB1 with microtubule-associated protein 2 (MAP2, neuron marker), glial fibrillary acid protein (GFAP, astrocyte marker), or ionized calcium binding adaptor molecule 1 (Iba1, microglia marker) was performed, respectively. Fixed brain was embedded in paraffin, and sections of 6 μm thick were used. The slices were soaked in limonene 2 times for 10 min each time, in 100% alcohol 2 times for 5 min each time, in 90% alcohol 2 times for 5 min each time and in distilled water (DW) for 3 min for deparaffinization. The slides were then soaked in 10 mM sodium citrate buffer (pH 6.0) in a heat-resistant container at autoclave unit at 120 degrees C for 10 min for antigen retrieval. After rinsing in running tap water for 5 min, the slides were washed by 0.025 % TBS-triton (TBS-T) 2 times for 5 min each time and incubated with 10% normal goat serum (NGS) containing 1% bovine serum albumin (BSA) in TBS for 2 h at room temperature. And then the slices were

incubated with primary antibodies; mouse anti-human HMGB1/HMG-1 antibody (1:100; R&D Systems, Minneapolis, MN, USA), rabbit anti-MAP2 antibody (1:500; Abcam, Cambridge, MA, USA), rabbit anti-GFAP antibody (1:1000; Novus Biologicals, Littleton, CO, USA) and rabbit anti-Iba1 antibody (1:250; Wako Pure Chemical Industries, Osaka, JAPAN) for 24 h at 4 degrees C, respectively. Corresponding secondary antibodies; Alexa fluor 555 F(ab') fragment of goat anti-mouse IgG (H+L) (1:500; Life Technologies, Grand Island, NY, USA) and FITC–conjugated affinity-purified donkey anti-rabbit IgG (H+L) (1:100; Jackson) for 1.5 h at 4 degrees C in a dark chamber after several rinse with TBS-T, followed by 4', 6-diamidino-2-phenylindole (DAPI, 0.5 mg/mL) for 5 min. The sections were then extensively washed with TBS-T and coverslipped.

Measurement of BBB leakage

To assess disruption of BBB, fluorescent immunostaining for rat albumin was performed. The slides after deparaffinization and antigen retrieval were incubated with 0.2% collagen in 10 mM TBS for 2 h at room temperature. Thereafter, the slides were incubated with sheep anti-rat albumin antibody (1:100; BETHYL, Montgomery, TX, USA) as a primary antibody and rabbit anti sheep IgG-heavy and light chain antibody conjugated to FITC (1:200; Jackson) as a secondary antibody. For the quantification, integration between signal intensity and the ratio of stained area to ipsilateral hemisphere were measured with Image J software

(NIH, Bethesda, USA) (Nakamura et al., 2013).

Morphological analyses

TH immunostaining

The density of TH-positive fibers in the striatum was determined and analyzed with a computerized analysis system as described previously (Shinko et al., 2014). Three sections at 0.5±1.0 mm anterior to the bregma were randomly selected for quantitative analyses. The two areas adjacent to the needle tract of lesioned side and the symmetrical areas in the contralateral side were analyzed, respectively. The percentages of lesion to the intact side were evaluated in each section and the averages were used for statistical analyses. The images were computer-processed into binary images using an appropriate threshold (Scion Image, Scion Corp., Frederick, MD, USA). The areas were then calculated and used for statistical analyses. The number of TH-positive neurons was counted of three sections at 4.8, 5.3, and 5.8 mm posterior to the bregma in the SNc, respectively. The percentage of the number of TH-positive neurons to the intact side was analyzed and the average was used for the statistical analyses.

Activation of microglia and astrocytes

The number of Iba1-positive cells and GFAP-positive cells in the striatum and SNc were counted in the two fixed areas (each 500 μm × 500 μm square) of three different sections which are the same level of corresponding to TH-immunostaining. The average of the data was

used for statistical analyses.

Western immunoblotting using brain homogenates

The levels of HMGB1 in the striatum and SNc were measured using a previously reported method (Zhang et al., 2011). Rat brain samples were collected at the time point of 1, 4 and 7 days after 6-OHDA injection. Brains were sliced at the thickness of 3 mm. The brain tissues of bilateral striatum and SNc were punched out using a biopsy punch (1.5 mm-hole, Kai corporation and Kai industries co., ltd, Japan) and homogenized in cold Radio Immuno Precipitation Assay buffer (RIPA, 150 mM NaCl, 0.1% Triton X-100, 0.5% sodium deoxycholate, 0.1% SDS, and 50 mM Tris-HCl, pH 8.0) with cocktail protease inhibitors (Sigma-Aldrich). The brain homogenates were then centrifuged at 10,000 g for 20 min. The supernatant mixed with western sample buffer was used. 20 μL of each sample was loaded to the SDS-PAGE. After transferring the proteins to a nitrocellulose membrane (Bio-Rad Laboratories, Inc., Hercules, CA, USA), the membranes were blocked with TBS-T and 10% skim milk, and then probed with the anti-HMGB1 mAb (#10-22) labeled by horseradish peroxidase using a Peroxidase Labeling Kit-NH2 (Dojindo Molecular Technologies, Inc., Kumamoto, Japan). β-actin was probed with a mouse anti-β-actin mAb (Santa Cruz Biotechnology, Inc., Santa Cruz, CA, USA) followed by a HRP conjugated goat anti-mouse Ab. After washing in TBS-T, an ECL system (Thermo Fisher Scientific Inc., Rockford, IL, USA)

was used to visualize the bands of HMGB1 and β-actin. Finally, the specific proteins on membranes were detected the specific protein using ImageQuant LAS 4000 mini (GE, Fairfield, CT, USA). For quantification of signals, the densities of specific bands were measured with Image J software. Specific bands for HMGB1 and β-actin were detected at 29 and 42 kDa, respectively.

Enzyme-linked immunosorbent assay (ELISA) of HMGB1 in plasma

For HMGB1 determination in plasma samples, blood samples (2 mL) were collected with EDTA preventing hemolysis through the heart under deep anesthesia with sodium pentobarbital (100 mg/kg, i.p.) followed by centrifugation at 3,000 rpm for 10 min at 4 degrees C. The supernatant was stored at -20 degrees C with protease inhibitor before use. HMGB1 was determined using a HMGB1 enzyme-linked immunosorbent assay kit (Shino-Test Co, Sagamihara, Japan) according to the manufacturer's protocol (Zhang et al., 2011).

Real time polymerase chain reaction (PCR)

The rats were injected with 50 mg/kg sodium pentobarbital (i.p.) at 1 and 4 days after 6-OHDA injection and then perfused transcardially with 200 ml of cold PBS before decapitation. Tissues corresponding to striatum (27 mm^3) and SNc (10 mm^3) were dissected. Total RNA was isolated with Bio-Robot EZ1 (QIAGEN, Hilden, Germany) according to the manufacturer's instructions. Total RNA (< 500 ng/μl) was reverse transcribed with Avian Myeloblastosis virus

reverse transcriptase XL and Oligo dT-primers (Takara RNA PCR Kit; Takara Biomedicals, Shiga, Japan). Using cDNA obtained by RT-PCR, real-time PCR was performed with the SYBR Premix EX *Taq* (Takara) in a Light Cycler instrument (Roche) according to the manufacturer's instructions. The sense and antisense primers used for the analysis of expression of mRNA were the following: Interleukin-1β (IL-1β), 5'-CACCTTCTTTTCCTTCATCTTTG-3' and 5'-GTCGTTGCTTGTCTCTCCTTGTA-3'; IL-6, 5'-GCCCTTCAGGAACAGCTATGA-3' and 5'-TGTCAACAACATCAGTCCCAAGA-3'; IL-8R, 5'-CATCCTGCCTCAGACCTATGG-3' and 5'-AAGACGAGGACCACAGCAAAG-3'; inducible nitric oxide synthase (iNOS), 5'-GCATCCCAAGTACGAGTGGT-3' and 5'-GAAGTCTCGGACTCCAATCTC-3'; tumor necrosis factor (TNF-α), 5'-GCCCAGACCCTCACACTC-3' and 5'-CCACTCCAGCTGCTCCTCT-3'; glyceraldehyde-3-phosphate dehydrogenase (GAPDH), 5'-AGCCCAGAACATCATCCCTG-3' and 5'-CACCACCTTCTTGATGTCATC-3'. The expression of GAPDH was used to normalize cDNA levels. The PCR products were analyzed by a melting curve to ascertain the specificity of amplification. The $2^{-\Delta\Delta CT}$ method was used to analyze the relative gene expression data (Livak and Schmittgen, 2001).

High-performance liquid chromatography (HPLC)

The contents of dopamine and its metabolites in the striatum were measured using a

previously reported method (Diaz-Corrales et al., 2012). All rats were injected with 50 mg/kg sodium pentobarbital (i.p.) at 14 days after 6-OHDA injection and then perfused transcardially with 200 ml of cold saline before decapitation. Striatum was dissected (35 cm^3), frozen in liquid nitrogen and stored until homogenization with 10 volumes of 200 mM ice-cold perchloric acid with 10 mM EDTA. Homogenized samples were centrifuged at 11,750 g for 20 min at 4 degrees C, and the supernatant was filtered (0.45 ml) and then injected directly into a high-performance liquid chromatography (HPLC) with electrochemical detectors (HPLC-ECD; Tosoh, Co., Tokyo, Japan). Regional concentrations of dopamine and the metabolites 3, 4-dihydroxyphenylacetic acid (DOPAC) were measured. The HPLC system consisted of a delivery pump (PX-8020; Tosoh, Co.) and an analytical column (EICOMPAK SC-5ODS, 3.0 × 150 mm; Eicom, Co., Kyoto, Japan). An electrochemical detector (EC-8020; Tosoh, Co.) with glassy carbon was used with a voltage setting of 700 mV and an Ag/AgCl reference electrode. A mobile phase containing 0.1 M citrate-sodium acetate buffer (pH 3.5), methanol (17% vol/vol), EDTA-2Na, and sodium 1-octanesulfonate was infused at a flow rate of 0.6 ml/min. Protein concentration was determined with a protein assay kit (Bio-Rad Laboratories, Hercules, CA, USA).

Statistical analyses

Statistical significance was evaluated by Student's *t*-test for comparisons between 2

groups, or by ANOVA with subsequent post hoc Scheffe's test for multiple comparisons. *P* values less than 0.05 were considered to be significant. Mean values are presented with standard error (SE).

Results

Anti-HMGB1 mAb reduces experimental PD symptoms

intravenous anti-HMGB1 mAb preserved TH-positive fibers in the striatum (anti-HMGB1 mAb group: 39.0±6.17%, and control mAb group: 21.6±4.66% relative to the intact side, Student *t*-test: p = 0.0243, each n = 9, Fig. 1A, C) and protected TH-positive dopaminergic neurons in the SNc against 6-OHDA neurotoxicity (anti-HMGB1 mAb group: 70.0±3.43%, and control mAb group: 56.1±2.42% relative to the intact side, Student *t*-test: p = 0.0071, each n = 9, Fig. 1B, D) compared to control mAb treated group (p's <0.05). Moreover, treatment with anti-HMGB1 mAb attenuated the 6-OHDA-induced reduction in striatal dopamine contents as revealed by HPLC at 14 days post-lesion (anti-HMGB1 mAb group: 28.4±1.96%, and control mAb group: 16.48±2.67% relative to the intact side, Student *t*-test: p = 0.0357, n = 4 in control mAb group and 3 in anti-HMGB1 mAb group, Fig. 2C).

The observed anti-HMGB1 mAb-mediated preservations of striatal dopaminergic fibers and SNc dopaminergic neurons were accompanied by amelioration of 6-OHDA-induced

motor deficits. Treatment with anti-HMGB1 mAb resulted in significant reduction in the contralateral bias as detected by cylinder test (anti-HMGB1 mAb group: 25.7±6.09 and -3.7±12.9%; control mAb group: 48.2±6.20 and 26.4±4.76%, Student *t*-test: p = 0.0305 and 0.038, at 7 and 14 days, respectively, each n = 9, Fig. 2A) and the number of amphetamine-induced rotations (anti-HMGB1 mAb group: 793.0±75.1 and 641.4±71.2; control mAb group: 1060±108.8 and 1040±137.8 turns/90 min, Student *t*-test; p = 0.0703 and 0.0276, at 7 and 14 days, respectively, each n = 9, Fig. 2B) compared to control mAb treated group (p's <0.05). Altogether, these results showed that anti-HMGB1 mAb preserved TH expression and dopamine levels in the nigrostriatal pathway and maintained motor function in 6-OHDA lesioned rats.

Treatment with anti-HMGB1 mAb suppresses upregulation of HMGB1 in plasma and brain tissue

To reveal that anti-HMGB1 mAb produced immunohistochemical, neurochemical and behavioral benefits by directly modulating HMGB1 levels, we next assessed the plasma and brain levels of HMGB1. Treatment with anti-HMGB1 mAb reduced HMGB1 levels in plasma as revealed by ELISA at 1, 4, 7, and 14 days after 6-OHDA injection, whereas the concentration of HMGB1 significantly increased during the same period in control mAb group (anti-HMGB1 mAb group: 2.08±0.68, 2.70±0.53, 2.27±0.53, and 1.13±0.06 ng/ml; control mAb group:

2.80±0.45, 4.47±0.76, 3.15±0.24, and 2.93±0.43 ng/ml, Student *t*-test: p = 0.477, 0.0317, 0.189, and 0.0122, at 1, 4, 7 and 14 days, respectively, n = 8 at day 4 and 7, n = 4 at day 1 and 14, Fig. 3A). With regard to brain tissue, the anti-HMGB1 mAb suppressed the increase of the expression of HMGB1 which gradually increased in the striatum and SNc in control mAb group at 1, 4 and 7 days (Striatum: anti-HMGB1 mAb group: 101.1±8.8, 113.2±12.9, and 112.2±47.2%, control mAb group: 115.6±10.5, 165.0±44.3, and 241.7±23.2% relative to the intact side, Student *t*-test: p=0.393, 0.379 and 0.0418, at 1, 4 and 7 days, respectively, n = 8 at day 4 and 7, n = 4 at day 1, SNc: anti-HMGB1 mAb group: 62.3±8.43 and 134.3±20.6%, control mAb group: 103.2±19.7 and 181.6±24.0% relative to the intact side, Student *t*-test: p = 0.243 and 0.139, at 4 and 7 days, respectively, each n = 4, Fig. 3B-D). These findings indicate that anti HMGB1 mAb inhibited the HMGB1 elevation in plasma and brain tissue produced by 6-OHDA lesion.

Cytoplastic and nuclear HMGB1 expression following anti-HMGB1 mAb treatment

HMGB1 striatal expression in MAP2-positive neurons and GFAP-positive astrocytes at day 1 and 7 post-lesion, respectively, moved from nucleus to the cytoplasm and the extracellular space in the control mAb group, whereas HMGB1 was retained into the nucleus in the anti-HMGB1 mAb group (Fig. 4A, B). HMGB1 in some astrocytes was retained in the nucleus, whereas HMGB1 in all neurons was released to extracellular space in control mAb

group. HMGB1 release from nucleus to cytoplasm from Iba1-positive microglia was not observed through all of the period in both groups (Fig. 4C). Of note, the increase of microglia was significantly inhibited in the anti-HMGB1 mAb group compared to the control mAb group in the striatum as well as SNc (anti-HMGB1 mAb group: 15.6±4.85 and 12.0±0.98, 30.8±2.54 and 13.6±1.19, 22.2±10.4 and 19.0±1.53, and 27.6±3.20 and 11.3±1.60, control mAb group: 10.0±4.85 and 11.0±1.0, 57.0±9.57 and 15.8±1.56, 66.3±3.86 and 31.5±5.64, and 55.5±15.2 and 29.5±1.60 cells/field of view in the striatum and SNc, at 1, 4, 7 and 14 days, respectively, Student *t*-test: p = 0.846 and 0.559, 0.0005 and 0.5322, 0.0009 and 0.0056, and 0.0047 and 0.0007 in the striatum and SNc, at 1, 4, 7 and 14 days, respectively, each n = 4, Fig. 5A-D). Furthermore, the treatment with anti-HMGB1 mAb maintained the shape of microglia in the unactivated state, whereas they were enlarged and become amoeboid in the control mAb group (Fig. 4C, 5A, C).

The increase in the number of astrocytes produced by 6-OHDA lesion was detected in both anti-HMGB1 mAb group and control mAb group in the striatum and SNc. There were no differences in the number of astrocytes between them except at 7 days after 6-OHDA lesion (anti-HMGB1 mAb group: 15.0±1.45 and 17.0±1.62, 30.4±3.00 and 22.5±3.42, 26.0±1.65 and 31.25±3.15, and 24.8±2.07 and 31±2.21, control mAb group: 17.0±1.75 and 16.8±1.88, 33±0.79 and 26.8±2.84, 35.5±1.11 and 38.0±2.81, and 29.2±3.36 and 28.5±2.49 cells/field of view in the

striatum and SNc, at 1, 4, 7 and 14 days, respectively, Student *t*-test: p = 0.4405 and 0.9334, 0.525 and 0.439, 0.0022 and 0.2152, and 0.3647 and 0.5392 in the striatum and SNc, at 1, 4, 7 and 14 days, respectively, each n = 4, Fig. 6A-D).

Treatment with anti-HMGB1 mAb inhibits BBB disruption in the striatum

Because BBB leakage has been shown to accompany 6-OHDA lesion, we next examined if BBB permeability was a downstream pathway solicited by anti-HMGB1 mAb. Treatment with anti-HMGB1 mAb remarkably suppressed disruption of BBB in the striatum at day 1 post-lesion as revealed by albumin immunostaining (anti-HMGB1 mAb group: 191±64.1, control mAb group: 1766±550 calculated as integration between signal intensity and the ratio of the stained area to ipsilateral hemispherere, Student *t*-test: p = 0.049, each n = 4, Fig. 7A, B). This set of data implicates that anti-HMGB1 mAb reduced the increased vascular permeability due to 6-OHDA neurotoxicity.

Treatment with anti-HMGB1 mAb inhibits inflammatory cytokines

Recognizing that BBB compromise is associated with inflammation after 6-OHDA lesion, we analyzed via RT-PCR the mRNA expression of inflammatory cytokines. Striatal, and to a lesser extent SNc mRNA expression of IL-1β and IL-6 increased at least 10-fold at day 1 and 4 post-lesion, respectively (IL-1β: anti-HMGB1 mAb group: 5.31±0.57 and 1.79±0.50, and 3.02±1.17 and 0.96±0.25, control mAb: 14.37±3.49 and 1.39±0.38, and 17.6±2.27 and

2.14±0.32 relative to the intact side in the striatum and SNc, at 1 and 4 days, respectively, IL-6: anti-HMGB1 mAb group: 2.29±0.57 and 1.45±0.29, and 0.85±0.36 and 0.50±0.21, control mAb: 1.70±0.54 and 1.02±0.15, and 12.7±8.94 and 2.68±0.81 relative to the intact side in the striatum and SNc, at 1 and 4 days, respectively, each n = 4, Fig. 8A, B). Treatment with anti-HMGB1 mAb significantly suppressed IL-1β in the striatum and SNc, and IL-6 in the striatum at day 4 post-lesion (IL-1β: Student *t*-test: p = 0.026 and 0.0214 at 4 days in the striatum and SNc, respectively, IL-6: Student *t*-test: p = 0.0319 and 0.0644 at 4 days in the striatum and SNc, respectively, Fig. 8A, B). There were no detectable treatment effects on cytokine mRNA expression at day 1 post-lesion (p>0.05), with no apparent effects of anti-HMGB1 mAb on the expression of iNOS, TNF-α and IL-8R (Fig. 8).

Discussion

We demonstrated for the first time that intravenous treatment with a neutralizing anti-HMGB1 mAb exerted neuroprotective effects on experimental PD induced by 6-OHDA injection into the right striatum of rats. The treatment with anti-HMGB1 mAb preserved TH-positive dopaminergic neurons in the SNc and TH-positive dopaminergic terminals and dopamine contents in the striatum. This therapeutic benefit on the nigrostriatal dopaminergic pathway was associated with a pronounced amelioration of 6-OHDA-mediated motor deficits.

This HMGB1 mAb significantly blocked the translocation of the HMGB1 from the nucleus to the cytoplasm of neurons and astrocytes, inhibited the increase of HMGB1 in plasma and the brain tissue, and subsequently conferred stabilization of BBB integrity coupled with anti-inflammatory effects.

HMGB1 and PD pathology

There are few reports implicating the role of HMGB1 in PD pathology. Because α-synuclein filaments specifically bind HMGB1, it has been speculated that such sequestration of the transcriptional cofactor HMGB1 may contribute to α-synuclein aggregation reminiscent of PD neurodegenerative process (Lindersson et al., 2004). Overexpression of α-synuclein binds to both cytosolic and nuclear HMGB1, impairs the cytosolic translocation of HMGB1, blocks HMGB1-BECN1 binding, in which beclin-1 is encoded, and leads to autophagy inhibition (Song et al., 2014). Moreover, a signaling axis with converging pathways of HMGB1-Mac1-NADPH oxidase serves as a secondary cell death bridge for chronic neuroinflammation to exacerbate progressive dopaminergic neurodegeneration (Gao et al., 2011). In the present study, anti-HMGB1 mAb retained HMGB1 in the nucleus and suppressed HMGB1 levels in plasma and the brain tissue which might have mediated the anti-inflammatory and anti-degenerative effects on the dopaminergic neuron. Altogether, these findings indicate that HMGB1 is likely a key cell death factor in the disease pathology and arresting HMGB1

poses as a new therapeutic target for PD.

Cellular dynamics of HMGB1 in PD

We demonstrated that nuclear HMGB1 translocated to the cytoplasm and partly to the extracellular space in neurons and astrocytes at day 1 and 7 post-lesion, respectively. This 6-OHDA-induced translocation of HMGB1 away from the nucleus preceded the elevation of HMGB1 in plasma and striatum. In contrast, anti-HMGB1 mAb sequestered the nuclear expression of HMGB1, as well as blocked the increase of HMGB1 in plasma and brain tissue. There are two main sources of extracellular HMGB1. The first route is discharge from the nuclei of necrotic cells and the second is secretion from immune cells such as macrophages and microglia (Gao et al., 2011; Wang et al., 1999). Under pathological CNS conditions, such as cerebral ischemia or subarachnoid hemorrhage, HMGB1 is secreted by astrocytes and neurons (Qiu et al., 2008; Shibasaki et al., 2010; Sun et al., 2014; Zhang et al., 2011). The secreted HMGB1 has been considered as a late inflammatory mediator following increased levels in TNF-α and β, and IL-1β in endotoxin lethality in mice (Wang et al., 1999), suggesting that secondary activated astrocyte mount a deleterious inflammatory response by secreting HMGB1. The present data showed that astrocytes appeared to release HMGB1 in the relatively later stage compared to secretion of HMGB1 by neurons, which partially reflected the cell death cascade seen in the previous reports. Our report further characterized the dynamics of HMGB1 secretion

by demonstrating a differential temporal pattern of HMGB1 release between astrocytes and neurons. Here, we showed that neurons secreted HMGB1 in the acute stage of 6-OHDA neurotoxicity accompanied by necrosis, whereas reactive astrocytes secreted HMGB1 at the later stage of neurodegeneration acting as a major trigger of inflammation-plagued secondary cell death. The increase of HMGB1 in plasma likely reflects HMGB1 released into the extracellular space as previously shown (Kim et al., 2006; Liu et al., 2007; Okuma et al., 2012). However, the cause of HMGB1 upregulation in brain tissue remains controversial. HMGB1 in the cerebral cortex peaked at day 1 after subarachnoid hemorrhage in rats (Sun et al., 2014). On the other hand, HMGB1 in the cerebral cortex and striatum decreased markedly at days 1 and 2 after middle cerebral artery occlusion ischemia in rats (Liu et al., 2007). HMGB1 signal is increased in the cytoplasm of reactive glia in spinal cord tissue of amyotrophic lateral sclerosis patients, which represents some aspects of neurodegeneration seen in PD (Casula et al., 2011). Although pathological conditions, lesion size, sampling methods and timing might affect the discrepant results, there is a general consensus among published studies that HMGB1 appears to be consistently elevated in brain tissues during chronic inflammation.

Anti-inflammatory action of anti-HMGB1 mAb

In the present study, anti-HMGB1 mAb inhibited microglial activation in the striatum and SNc at day 4 after 6-OHDA injection. Anti-HMGB1 mAb also decreased the number of

reactive astrocytes at day 7 post-lesion in the striatum, although the effects on microglial activation at this time point were more prominent. Many reports have demonstrated that microglial cells are involved in neuroinflammation in PD (Hirsch and Hunot, 2009; More et al., 2013), in particular microglial activation, in concert with oxidative stress and apoptosis contributes to degeneration of dopaminergic neurons (Pabon et al., 2011; Saura et al., 2003). Similarly, a critical function of reactive astrocytes has been ascribed partly to the inflammatory reaction that occurs in the SNc in PD (Lee et al., 2010; Miklossy et al., 2006). For example, the presence of intercellular adhesion molecule-1 (ICAM-1)-positive reactive astrocytes in PD patients and MPTP-treated monkeys is indicative of a proinflammatory process (Miklossy et al., 2006). On the other hand, astrocytes are also known as major source of a number of neurotrophic factors, such as glial cell-line-derived neurotrophic factor (GDNF) (Chen et al., 2006; Lin et al., 1993) and brain-derived neurotrophic factor (BDNF) (Chen et al., 2006; Knott et al., 2002), both of which have been shown to be neuroprotective to dopaminergic neurons. Following 6-OHDA lesion in the present study, reactive astrocytes were shown to release HMGB1 which might have propelled neuroinflammatory effects, in conjunction with 6-OHDA's neurotoxicity, on dopaminergic neurons. In view of our observed inhibition of activated microglial cells and reactive astrocytes accompanying the anti-inflammatory response, a better understanding of PD neuroinflammation will further clarify the mechanism of action of

anti-HMGB1 mAb and optimize its therapeutic benefits against dopaminergic depletion.

Anti-HMGB1 mAb suppresses inflammatory cytokines including IL-1β and IL-6

In this study, the involvement of significant upregulation of IL-6 and IL-1β in the neuroinflammation on rat model of PD was shown. In characterizing downstream anti-inflammatory effects of anti-HMGB1 mAb, we showed that anti-HMGB1 mAb suppressed the increase of IL-1β and IL-6 in the striatum and IL-1β in the SNc relative to contralateral side at day 4 after 6-OHDA lesion. However, other inflammation-related molecules such as IL-8R, TNF-α or iNOS were not suppressed by this antibody treatment. Most studies indicated that HMGB1 could elicit the upregulation of various cytokines. HMGB1 stimulated microglial cells to release inflammatory and neurotoxic factors, including TNF-α, IL-1β and nitric oxide in the co-culture of neurons and astrocytes (Gao et al., 2011). Stimulation with HMGB1 in complex with lipopolysaccharide, IL-1α or IL-1β enhanced production of TNF, IL-6 and IL-8 from synovial fibroblasts (Wahamaa et al., 2011). That anti-HMGB1 mAb could partially block the 6-OHDA-induced inflammatory cascade offers further evidence that HMGB1 may be a key molecule in the inflammation-mediated cell death in PD.

Anti-HMGB1 mAb ameliorates BBB disruption

Inflammation may also initiate BBB leakage in PD (More et al., 2013). Here, we demonstrated that anti-HMGB1 mAb attenuated the 6-OHDA-induced BBB disruption in the

striatum. Recombinant human HMGB1 elicited pro-inflammatory responses on endothelial cells in vitro, which subsequently induced increased vascular permeability, cell swelling and loss of barrier function (Fiuza et al., 2003). Anti-HMGB1 antibody inhibited the swelling of astrocytic end-feet surrounding vascular endothelial cells and reduced brain edema in ischemia and brain traumatic injury (Okuma et al., 2012; Zhang et al., 2011). But little is known about arresting the BBB disruption as treatment target for PD. Circulating serum-derived inflammatory molecules that penetrate the brain due to increased permeability of BBB may activate microglial cells (Ransohoff and Perry, 2009). Additionally, in the midbrain of PD patients, uptake of [11C]-verapamil was elevated as revealed by positron emission tomography, which implies a dysfunctional BBB as a likely causative factor in PD (Kortekaas et al., 2005). In tandem with direct reduction of cytokines in the brain, anti-HMGB1 mAb might have also suppressed the CNS entry of peripheral inflammatory molecules by ameliorating the 6-OHDA-induced BBB disruption.

Chronic inflammation is an important pathological feature of PD that may allow innovative disease therapeutic intervention. In the present study, we indicated that HMGB1 plays a major role in 6-OHDA-induced inflammation, and that the treatment with anti-HMGB1 mAb exerted neuroprotective effects possibly via inhibition of this inflammatory response to 6-OHDA neurotoxicity (Fig. 9).

References

Andrassy, M., Volz, H.C., Igwe, J.C., Funke, B., Eichberger, S.N., Kaya, Z., Buss, S., Autschbach, F., Pleger, S.T., Lukic, I.K., Bea, F., Hardt, S.E., Humpert, P.M., Bianchi, M.E., Mairbaurl, H., Nawroth, P.P., Remppis, A., Katus, H.A., Bierhaus, A., 2008. High-mobility group box-1 in ischemia-reperfusion injury of the heart. Circulation 117, 3216-3226.

Casula, M., Iyer, A.M., Spliet, W.G., Anink, J.J., Steentjes, K., Sta, M., Troost, D., Aronica, E., 2011. Toll-like receptor signaling in amyotrophic lateral sclerosis spinal cord tissue. Neuroscience 179, 233-243.

Chen, P.S., Peng, G.S., Li, G., Yang, S., Wu, X., Wang, C.C., Wilson, B., Lu, R.B., Gean, P.W., Chuang, D.M., Hong, J.S., 2006. Valproate protects dopaminergic neurons in midbrain neuron/glia cultures by stimulating the release of neurotrophic factors from astrocytes. Molecular psychiatry 11, 1116-1125.

Cicchetti, F., Brownell, A.L., Williams, K., Chen, Y.I., Livni, E., Isacson, O., 2002. Neuroinflammation of the nigrostriatal pathway during progressive 6-OHDA dopamine degeneration in rats monitored by immunohistochemistry and PET imaging. The European journal of neuroscience 15, 991-998.

Depino, A.M., Earl, C., Kaczmarczyk, E., Ferrari, C., Besedovsky, H., del Rey, A., Pitossi, F.J., Oertel, W.H., 2003. Microglial activation with atypical proinflammatory cytokine expression in

a rat model of Parkinson's disease. The European journal of neuroscience 18, 2731-2742.

Diaz-Corrales, F.J., Miyazaki, I., Asanuma, M., Ruano, D., Rios, R.M., 2012. Centrosomal aggregates and Golgi fragmentation disrupt vesicular trafficking of DAT. Neurobiology of aging 33, 2462-2477.

Fiuza, C., Bustin, M., Talwar, S., Tropea, M., Gerstenberger, E., Shelhamer, J.H., Suffredini, A.F., 2003. Inflammation-promoting activity of HMGB1 on human microvascular endothelial cells. Blood 101, 2652-2660.

Gao, H.M., Zhou, H., Zhang, F., Wilson, B.C., Kam, W., Hong, J.S., 2011. HMGB1 acts on microglia Mac1 to mediate chronic neuroinflammation that drives progressive neurodegeneration. The Journal of neuroscience , 1081-1092.

Hamada, T., Torikai, M., Kuwazuru, A., Tanaka, M., Horai, N., Fukuda, T., Yamada, S., Nagayama, S., Hashiguchi, K., Sunahara, N., Fukuzaki, K., Nagata, R., Komiya, S., Maruyama, I., Fukuda, T., Abeyama, K., 2008. Extracellular high mobility group box chromosomal protein 1 is a coupling factor for hypoxia and inflammation in arthritis. Arthritis and rheumatism 58, 2675-2685.

He, Y., Appel, S., Le, W., 2001. Minocycline inhibits microglial activation and protects nigral cells after 6-hydroxydopamine injection into mouse striatum. Brain research 909, 187-193.

Hirsch, E.C., Hunot, S., 2009. Neuroinflammation in Parkinson's disease: a target for

neuroprotection? Lancet neurology 8, 382-397.

Imamura, K., Hishikawa, N., Sawada, M., Nagatsu, T., Yoshida, M., Hashizume, Y., 2003. Distribution of major histocompatibility complex class II-positive microglia and cytokine profile of Parkinson's disease brains. Acta neuropathologica 106, 518-526.

Kawabata, H., Setoguchi, T., Yone, K., Souda, M., Yoshida, H., Kawahara, K., Maruyama, I., Komiya, S., 2010. High mobility group box 1 is upregulated after spinal cord injury and is associated with neuronal cell apoptosis. Spine 35, 1109-1115.

Kim, J.B., Sig Choi, J., Yu, Y.M., Nam, K., Piao, C.S., Kim, S.W., Lee, M.H., Han, P.L., Park, J.S., Lee, J.K., 2006. HMGB1, a novel cytokine-like mediator linking acute neuronal death and delayed neuroinflammation in the postischemic brain. The Journal of neuroscience : the official journal of the Society for Neuroscience 26, 6413-6421.

Knott, C., Stern, G., Kingsbury, A., Welcher, A.A., Wilkin, G.P., 2002. Elevated glial brain-derived neurotrophic factor in Parkinson's diseased nigra. Parkinsonism & related disorders 8, 329-341.

Kortekaas, R., Leenders, K.L., van Oostrom, J.C., Vaalburg, W., Bart, J., Willemsen, A.T., Hendrikse, N.H., 2005. Blood-brain barrier dysfunction in parkinsonian midbrain in vivo. Annals of neurology 57, 176-179.

Lee, H.J., Suk, J.E., Patrick, C., Bae, E.J., Cho, J.H., Rho, S., Hwang, D., Masliah, E., Lee, S.J.,

2010. Direct transfer of alpha-synuclein from neuron to astroglia causes inflammatory responses in synucleinopathies. The Journal of biological chemistry 285, 9262-9272.

Lin, L.F., Doherty, D.H., Lile, J.D., Bektesh, S., Collins, F., 1993. GDNF: a glial cell line-derived neurotrophic factor for midbrain dopaminergic neurons. Science (New York, N.Y.) 260, 1130-1132.

Lindersson, E.K., Hojrup, P., Gai, W.P., Locker, D., Martin, D., Jensen, P.H., 2004. alpha-Synuclein filaments bind the transcriptional regulator HMGB-1. Neuroreport 15, 2735-2739.

Liu, K., Mori, S., Takahashi, H.K., Tomono, Y., Wake, H., Kanke, T., Sato, Y., Hiraga, N., Adachi, N., Yoshino, T., Nishibori, M., 2007. Anti-high mobility group box 1 monoclonal antibody ameliorates brain infarction induced by transient ischemia in rats. FASEB journal : official publication of the Federation of American Societies for Experimental Biology 21, 3904-3916.

Livak, K.J., Schmittgen, T.D., 2001. Analysis of relative gene expression data using real-time quantitative PCR and the 2(-Delta Delta C(T)) Method. Methods (San Diego, Calif.) 25, 402-408.

Lotze, M.T., Tracey, K.J., 2005. High-mobility group box 1 protein (HMGB1): nuclear weapon in the immune arsenal. Nature reviews. Immunology 5, 331-342.

McGeer, P.L., Itagaki, S., Boyes, B.E., McGeer, E.G., 1988. Reactive microglia are positive for HLA-DR in the substantia nigra of Parkinson's and Alzheimer's disease brains. Neurology 38, 1285-1291.

Miklossy, J., Doudet, D.D., Schwab, C., Yu, S., McGeer, E.G., McGeer, P.L., 2006. Role of ICAM-1 in persisting inflammation in Parkinson disease and MPTP monkeys. Experimental neurology 197, 275-283.

More, S.V., Kumar, H., Kim, I.S., Song, S.Y., Choi, D.K., 2013. Cellular and molecular mediators of neuroinflammation in the pathogenesis of Parkinson's disease. Mediators of inflammation 2013, 952375.

Nakamura, Y., Morioka, N., Abe, H., Zhang, F.F., Hisaoka-Nakashima, K., Liu, K., Nishibori, M., Nakata, Y., 2013. Neuropathic pain in rats with a partial sciatic nerve ligation is alleviated by intravenous injection of monoclonal antibody to high mobility group box-1. PloS one 8, e73640.

Okuma, Y., Liu, K., Wake, H., Zhang, J., Maruo, T., Date, I., Yoshino, T., Ohtsuka, A., Otani, N., Tomura, S., Shima, K., Yamamoto, Y., Yamamoto, H., Takahashi, H.K., Mori, S., Nishibori, M., 2012. Anti-high mobility group box-1 antibody therapy for traumatic brain injury. Annals of neurology 72, 373-384.

Pabon, M.M., Bachstetter, A.D., Hudson, C.E., Gemma, C., Bickford, P.C., 2011. CX3CL1

reduces neurotoxicity and microglial activation in a rat model of Parkinson's disease. Journal of neuroinflammation 8, 9.

Park, J.S., Svetkauskaite, D., He, Q., Kim, J.Y., Strassheim, D., Ishizaka, A., Abraham, E., 2004. Involvement of toll-like receptors 2 and 4 in cellular activation by high mobility group box 1 protein. The Journal of biological chemistry 279, 7370-7377.

Qiu, J., Nishimura, M., Wang, Y., Sims, J.R., Qiu, S., Savitz, S.I., Salomone, S., Moskowitz, M.A., 2008. Early release of HMGB-1 from neurons after the onset of brain ischemia. Journal of cerebral blood flow and metabolism 28, 927-938.

Raman, K.G., Sappington, P.L., Yang, R., Levy, R.M., Prince, J.M., Liu, S., Watkins, S.K., Schmidt, A.M., Billiar, T.R., Fink, M.P., 2006. The role of RAGE in the pathogenesis of intestinal barrier dysfunction after hemorrhagic shock. American journal of physiology. Gastrointestinal and liver physiology 291, G556-565.

Ransohoff, R.M., Perry, V.H., 2009. Microglial physiology: unique stimuli, specialized responses. Annual review of immunology 27, 119-145.

Roof, R.L., Schielke, G.P., Ren, X., Hall, E.D., 2001. A comparison of long-term functional outcome after 2 middle cerebral artery occlusion models in rats. Stroke; a journal of cerebral circulation 32, 2648-2657.

Saura, J., Pares, M., Bove, J., Pezzi, S., Alberch, J., Marin, C., Tolosa, E., Marti, M.J., 2003.

Intranigral infusion of interleukin-1beta activates astrocytes and protects from subsequent 6-hydroxydopamine neurotoxicity. Journal of neurochemistry 85, 651-661.

Sawa, H., Ueda, T., Takeyama, Y., Yasuda, T., Shinzeki, M., Nakajima, T., Kuroda, Y., 2006. Blockade of high mobility group box-1 protein attenuates experimental severe acute pancreatitis. World journal of gastroenterology : WJG 12, 7666-7670.

Schallert, T., Fleming, S.M., Leasure, J.L., Tillerson, J.L., Bland, S.T., 2000. CNS plasticity and assessment of forelimb sensorimotor outcome in unilateral rat models of stroke, cortical ablation, parkinsonism and spinal cord injury. Neuropharmacology 39, 777-787.

Shibasaki, M., Sasaki, M., Miura, M., Mizukoshi, K., Ueno, H., Hashimoto, S., Tanaka, Y., Amaya, F., 2010. Induction of high mobility group box-1 in dorsal root ganglion contributes to pain hypersensitivity after peripheral nerve injury. Pain 149, 514-521.

Shichita, T., Hasegawa, E., Kimura, A., Morita, R., Sakaguchi, R., Takada, I., Sekiya, T., Ooboshi, H., Kitazono, T., Yanagawa, T., Ishii, T., Takahashi, H., Mori, S., Nishibori, M., Kuroda, K., Akira, S., Miyake, K., Yoshimura, A., 2012. Peroxiredoxin family proteins are key initiators of post-ischemic inflammation in the brain. Nat Med 18, 911-917.

Shinko, A., Agari, T., Kameda, M., Yasuhara, T., Kondo, A., Tayra, J.T., Sato, K., Sasaki, T., Sasada, S., Takeuchi, H., Wakamori, T., Borlongan, C.V., Date, I., 2014. Spinal Cord Stimulation Exerts Neuroprotective Effects against Experimental Parkinson's Disease. PloS one

9, e101468.

Song, J.X., Lu, J.H., Liu, L.F., Chen, L.L., Durairajan, S.S., Yue, Z., Zhang, H.Q., Li, M., 2014. HMGB1 is involved in autophagy inhibition caused by SNCA/alpha-synuclein overexpression: a process modulated by the natural autophagy inducer corynoxine B. Autophagy 10, 144-154.

Sun, Q., Wu, W., Hu, Y.C., Li, H., Zhang, D., Li, S., Li, W., Li, W.D., Ma, B., Zhu, J.H., Zhou, M.L., Hang, C.H., 2014. Early release of high-mobility group box 1 (HMGB1) from neurons in experimental subarachnoid hemorrhage in vivo and in vitro. Journal of neuroinflammation 11, 106.

Tsung, A., Tohme, S., Billiar, T.R., 2014. High mobility group box-1 in sterile inflammation. Journal of internal medicine.

Wahamaa, H., Schierbeck, H., Hreggvidsdottir, H.S., Palmblad, K., Aveberger, A.C., Andersson, U., Harris, H.E., 2011. High mobility group box protein 1 in complex with lipopolysaccharide or IL-1 promotes an increased inflammatory phenotype in synovial fibroblasts. Arthritis research & therapy 13, R136.

Wang, H., Bloom, O., Zhang, M., Vishnubhakat, J.M., Ombrellino, M., Che, J., Frazier, A., Yang, H., Ivanova, S., Borovikova, L., Manogue, K.R., Faist, E., Abraham, E., Andersson, J., Andersson, U., Molina, P.E., Abumrad, N.N., Sama, A., Tracey, K.J., 1999. HMG-1 as a late mediator of endotoxin lethality in mice. Science (New York, N.Y.) 285, 248-251.

Yang, H., Ochani, M., Li, J., Qiang, X., Tanovic, M., Harris, H.E., Susarla, S.M., Ulloa, L., Wang, H., DiRaimo, R., Czura, C.J., Wang, H., Roth, J., Warren, H.S., Fink, M.P., Fenton, M.J., Andersson, U., Tracey, K.J., 2004. Reversing established sepsis with antagonists of endogenous high-mobility group box 1. Proceedings of the National Academy of Sciences of the United States of America 101, 296-301.

Yang, R., Harada, T., Mollen, K.P., Prince, J.M., Levy, R.M., Englert, J.A., Gallowitsch-Puerta, M., Yang, L., Yang, H., Tracey, K.J., Harbrecht, B.G., Billiar, T.R., Fink, M.P., 2006. Anti-HMGB1 neutralizing antibody ameliorates gut barrier dysfunction and improves survival after hemorrhagic shock. Molecular medicine (Cambridge, Mass.) 12, 105-114.

Yasuda, T., Ueda, T., Takeyama, Y., Shinzeki, M., Sawa, H., Nakajima, T., Ajiki, T., Fujino, Y., Suzuki, Y., Kuroda, Y., 2006. Significant increase of serum high-mobility group box chromosomal protein 1 levels in patients with severe acute pancreatitis. Pancreas 33, 359-363.

Zhang, J., Takahashi, H.K., Liu, K., Wake, H., Liu, R., Maruo, T., Date, I., Yoshino, T., Ohtsuka, A., Mori, S., Nishibori, M., 2011. Anti-high mobility group box-1 monoclonal antibody protects the blood-brain barrier from ischemia-induced disruption in rats. Stroke; a journal of cerebral circulation 42, 1420-1428.

Figure Legends

Figure 1: The treatment with anti-HMGB1 mAb preserves TH-positive fibers in the striatum and TH-positive neurons in the SNc.

A: TH-positive fibers in the striatum on rat model of PD received the treatment with anti-HMGB1 mAb (right) and control mAb (left) are shown (left scale bar: 5 mm, right: 300 μm). ***B***: TH-positive neurons in the SNc on rat model of PD received the treatment with anti-HMGB1 mAb (lower) and control mAb (upper) at three different coronal levels are shown (left: rostral region, center: medial region, right: caudal region, scale bar: 300 μm). ***C***: The ratio to the intact side of TH-positive fibers was analyzed using a computerized image analysis system. TH-positive fibers in the striatum significantly preserved in the treatment with anti-HMGB mAb compared to control mAb group (each n = 9, the mean ± SEM, *$p<0.05$). ***D***: The ratio to the intact side of TH-positive neurons in the SNc was analyzed. TH-positive neurons in the SNc significantly preserved in the treatment with anti-HMGB mAb compared to control mAb group (each n = 9, the mean ± SEM, **$p<0.01$).

Figure 2: The treatment with anti-HMGB1 mAb ameliorates 6-OHDA-induced motor deficits and preserves striatal dopamine contents.

A, ***B***: The results of contralateral bias in the cylinder test (***A***) and the number of amphetamine-induced rotations per 90 min (***B***) are shown. The treatment with anti-HMGB1

mAb significantly ameliorates 6-OHDA-induced motor deficits compared to control mAb group (each n = 9, the mean ± SEM, *p<0.05).

C, ***D***: The ratio to the intact side of striatal dopamine (***C***) and DOPAC (***D***) contents at day 14 after 6-OHDA injection are shown. Treatment with Anti-HMGB1 mAb significantly preserved striatal dopamine contents compared to the control mAb treated group (n = 4 in control mAb group and 3 in anti-HMGB1 mAb group, the mean ± SEM, *p<0.05).

Figure 3: The treatment with anti-HMGB1 mAb suppresses the increase of HMGB1 in plasma and brain tissue.

A: Blood samples were collected at day 1, 4, 7, and 14 after 6-OHDA injection, respectively and evaluated by ELISA. HMGB1 significantly increased at day 4 and 7 in control mAb group. Anti-HMGB1 mAb significantly suppresses the increase of HMGB1 in plasma compared to control mAb group at day 4 and 14 (n = 8 at day 4 and 7, n = 4 at day 1 and 14, the mean ± SEM, #p<0.05, ##p<0.01 evaluated by ANOVA with subsequent post hoc Scheffe's test, *p<0.05, **p<0.01 compared to control mAb group, respectively). ***B***: Brain tissues in the striatum and SNc were collected at 1, 4 and 7 days, respectively and examined by western immunoblotting. The expression of HMGB1 (29kD) and β-actin (42kD) are shown, respectively. ***C***: The ratio to the intact side of expression of HMGB1 in the striatum is shown. The treatment with anti-HMGB1 mAb suppressed the increase of HMGB1 in the striatal tissue, whereas

HMGB1 gradually increased in control mAb group (n = 8 at day 4 and 7, n = 4 at day 1, the mean ± SEM, *p<0.05). ***D***: The ratio to the intact side of expression of HMGB1 in the SNc at 4 and 7 days is shown. The treatment with anti-HMGB1 mAb likely suppresses the increase of HMGB1 in the SNc (each n = 4, the mean ± SEM).

Figure 4: HMGB1 is released from neurons and astrocytes in the striatum by immunohistochemical investigations.

A: Distributions of HMGB1 (red) in MAP2-positive neurons (green) in control mAb group (upper) and anti-HMGB1 mAb group (lower) at day 1 after 6-OHDA injection are shown. HMGB1 was translocated from the nuclear compartment and moved to extracellular space in control mAb group, whereas it was retained in the nucleus in anti-HMGB1 group. ***B***: Distributions of HMGB1 in GFAP-positive astrocytes (green) in the control mAb group (upper) and the anti-HMGB1 mAb group (lower) at day 7 are shown. HMGB1 in some astrocytes was moved to the cytoplasm in control mAb group. ***C***: Distribution of HMGB1 in Iba1-positive microglia (green) in the control mAb group (upper) and the anti-HMGB1 mAb group (lower) at day 4 is shown. HMGB1 in activated microglia was retained in the nucleus in control mAb group as well as in anti-HMGB1 mAb group (scale bar; 50 μm, magnified images: 20 μm).

Figure 5: The treatement with anti-HMGB1 mAb inhibits proliferation of microglia both in the striatum and SNc.

A, ***C***: Iba1 stainings in the striatum (***A***) and the SNc (***C***) at day 1, 4, 7 and 14, respectively after 6-OHDA injection are shown. In control mAb group, the number of microglia increased at day 4 and the shape of microglia was enlarged and become amoeboid in the striatum and the SNc. The treatment with anti-HMGB1 mAb inhibited the proliferation and activation of microglia in the striatum and SNc compared to control mAb group and kept inactive state. ***B***, ***D***: The quantifications of the number of Iba1-positive microglia at three different coronal sections are shown (each n = 4, the mean ± SEM, #p<0.05, ##p<0.01, ###p<0.001 evaluated by ANOVA with subsequent post hoc Scheffe's test, *p<0.05, **p<0.01 compared to control mAb group, respectively).

Figure 6: The astrocytes proliferated in the striatum and the SNc by 6-OHDA injection.

A, C: GFAP stainings in the striatum (***A***) and the SNc (***C***) at day 1, 4, 7 and 14 after 6-OHDA injection are shown, respectively. In both anti-HMGB1 mAb group and control mAb group, the number of astrocytes was increased in the striatum and lately SNc. There were no differences about the number of astrocytes between them except at 7 days. ***B, D***: The quantifications of the number of GFAP-positive astrocytes at three different coronal sections are shown (each n = 4, the mean ± SEM, #p<0.05, ##p<0.01, ###p<0.001 evaluated by ANOVA with subsequent post hoc Scheffe's test, **p<0.01 compared to control mAb group, respectively).

Figure 7: The treatment with anti-HMGB1 mAb inhibits disruption of BBB in the

striatum.

A: Fluorescent immunostainings for rat albumin at day 1 after 6-OHDA injection are shown (scale bar: 5 mm). ***B***: The quantification using a computerized image analysis system at three different coronal sections is shown. The treatment with anti-HMGB1 mAb significantly suppressed disruption of BBB compared to control mAb group. (each n = 4, the mean ± SEM, *p<0.05).

Figure 8: The treatment with anti-HMGB1 mAb inhibits the upregulation of inflammation-related cytokines including IL-1β and IL-6.

A, ***B:*** The samples were collected in the striatum and SNc at day 1 and 4 after 6-OHDA injection and analyzed with RT-PCR. The ratio to the intact side of expression of inflammation-related cytokines including IL-1β, IL-6, IL-8R, TNF-α, and iNOS in the striatum (***A***) and SNc (***B***) are shown, respectively. The treatment with anti-HMGB1 mAb suppressed IL-6 and IL-1β in the striatum at day 4 and IL-1β in the SNc at day 4 (each n = 4, the mean ± SEM, *p<0.05, **p<0.01).

Figure 9: The possible mechanism of neuroprotective effects by anti-HMGB1 mAb in this study.

In this study, HMGB1 released from neurons and astrocytes activates microglia and astrocytes with subsequent induction of neuroinflammation followed by neuronal death. The neuronal cells

releasing all HMGB1 might be fated to cell death. However immune cells including reactive astrocytes partly release HMGB1 might survive. Alternatively, increased disruption of BBB with the leakage of serum constituents from vessels might be involved in the pathogenesis of PD. Anti-HMGB1 mAb successfully inhibits HMGB1 translocation from nucleus to cytoplasm and extracellular space, increase of HMGB1 in plasma and brain tissue, and disruption of BBB followed by neuroinflammation.

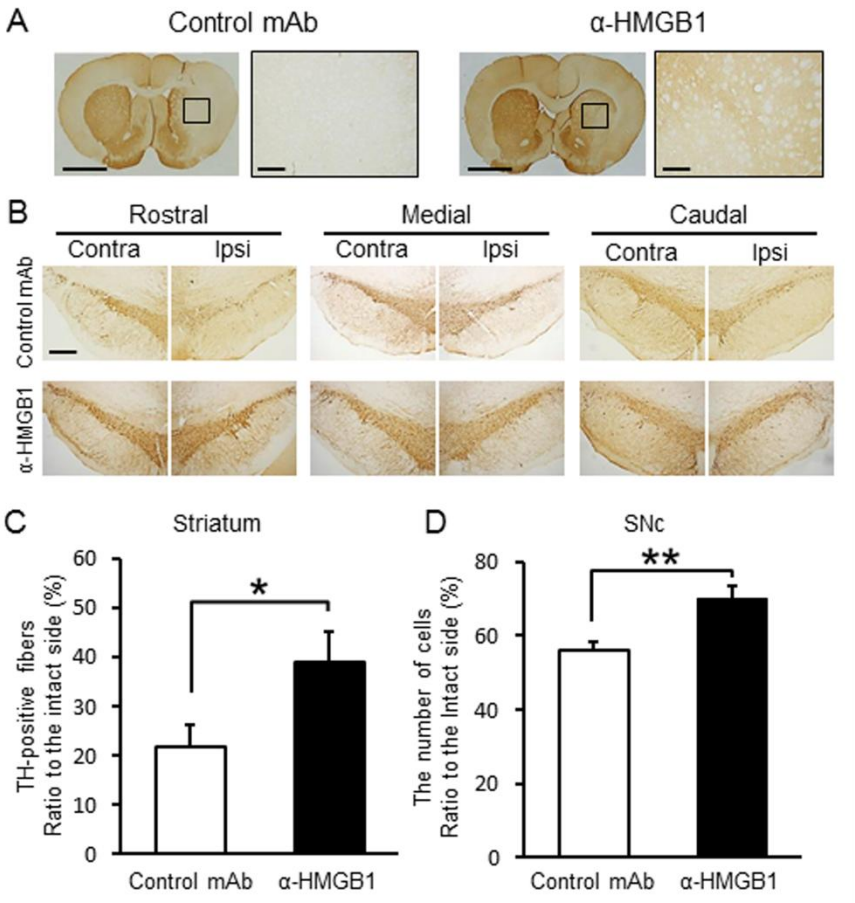

Fig. 1

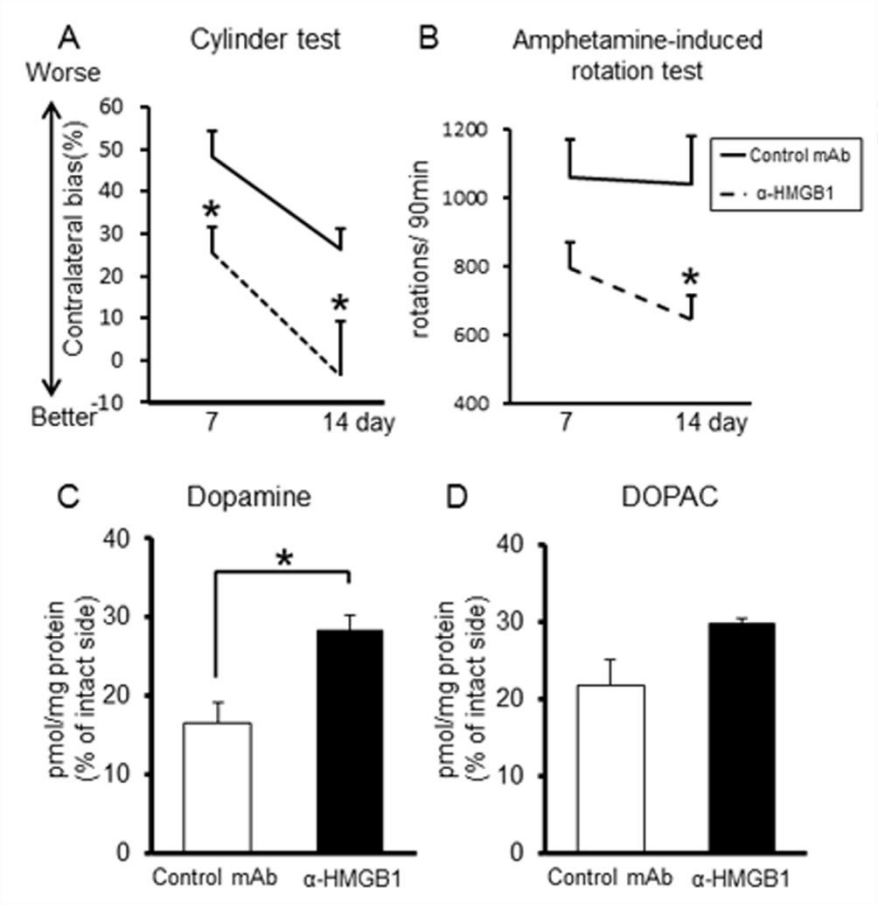

Fig. 2

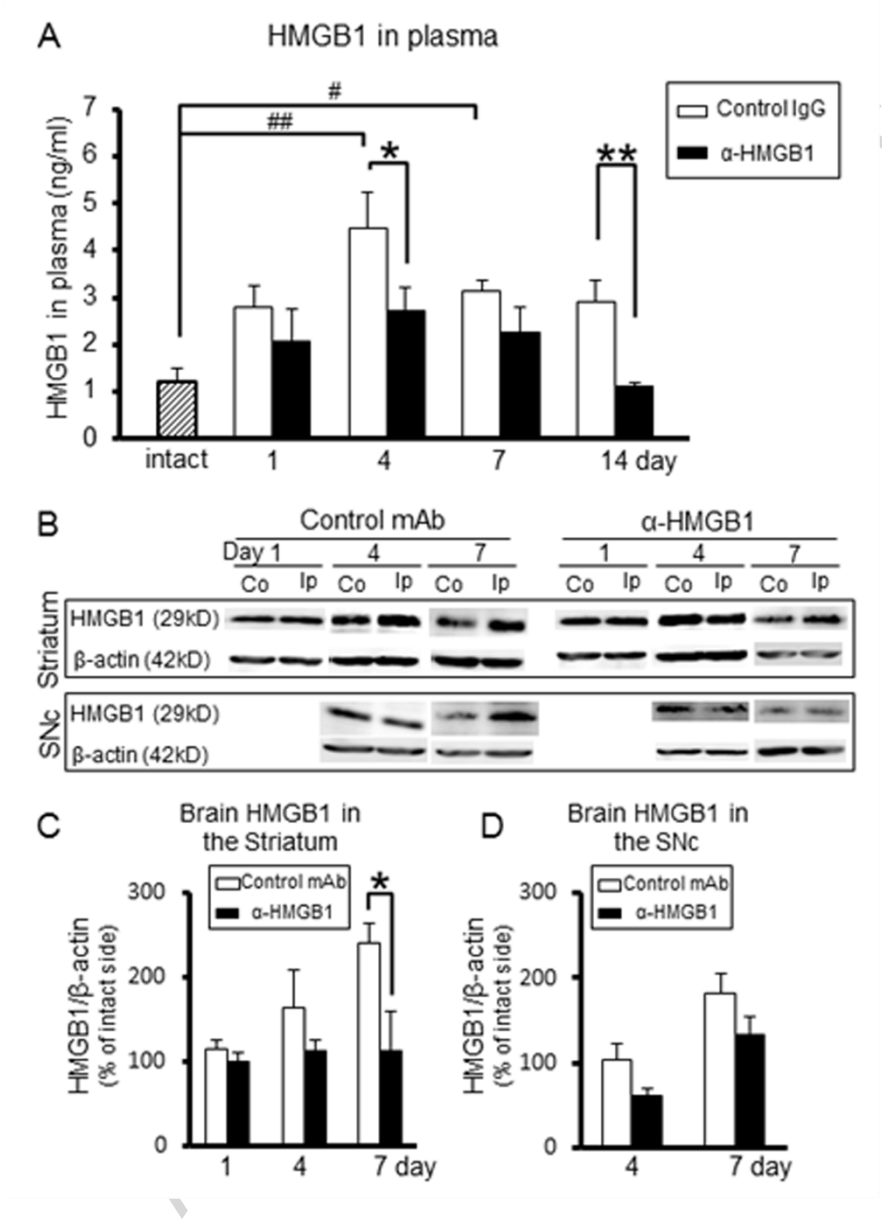

Fig. 3

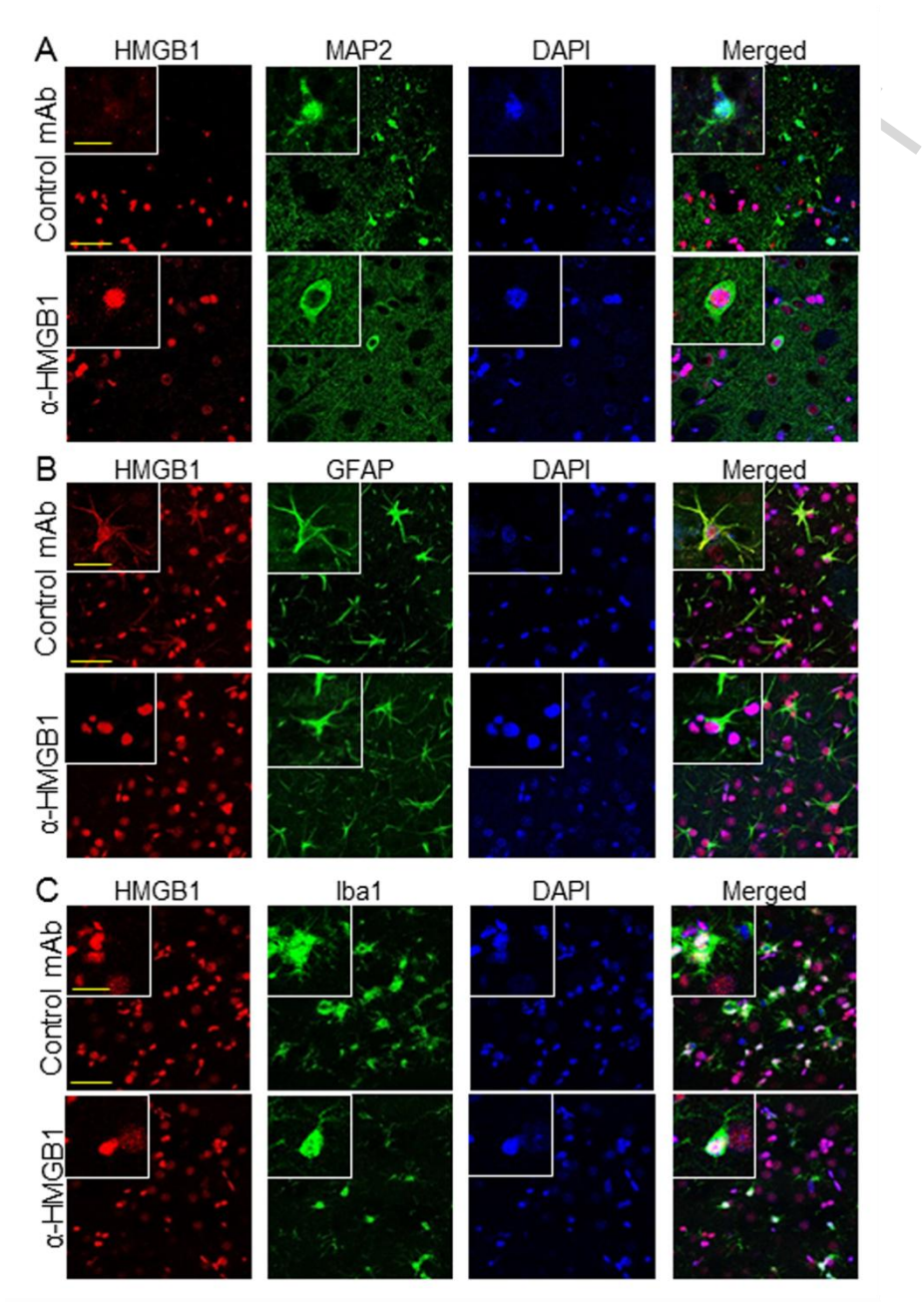

Fig. 4

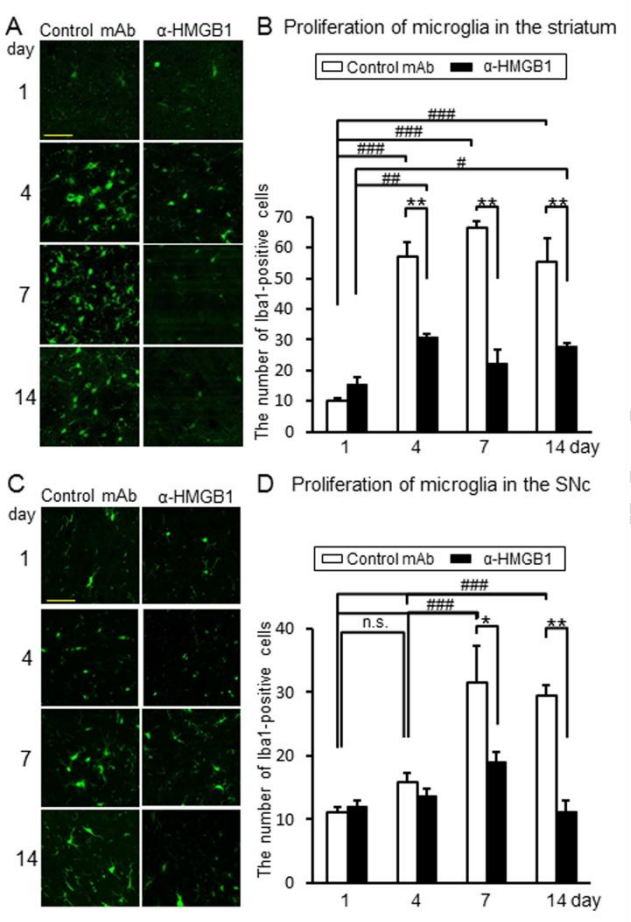

Fig. 5

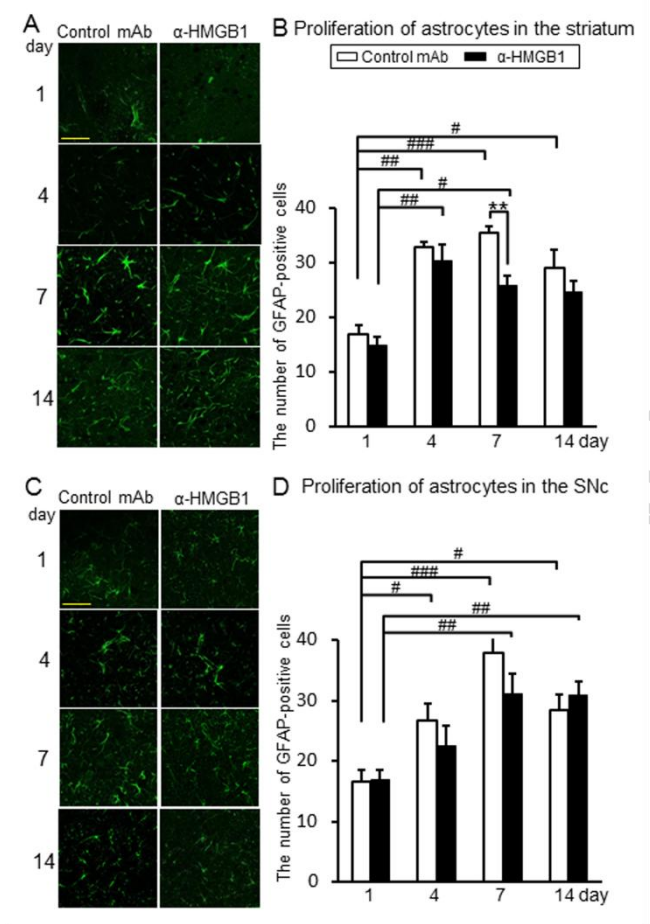

Fig. 6

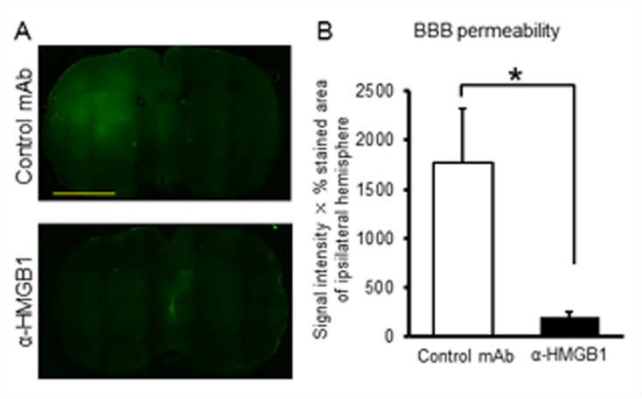

Fig. 7

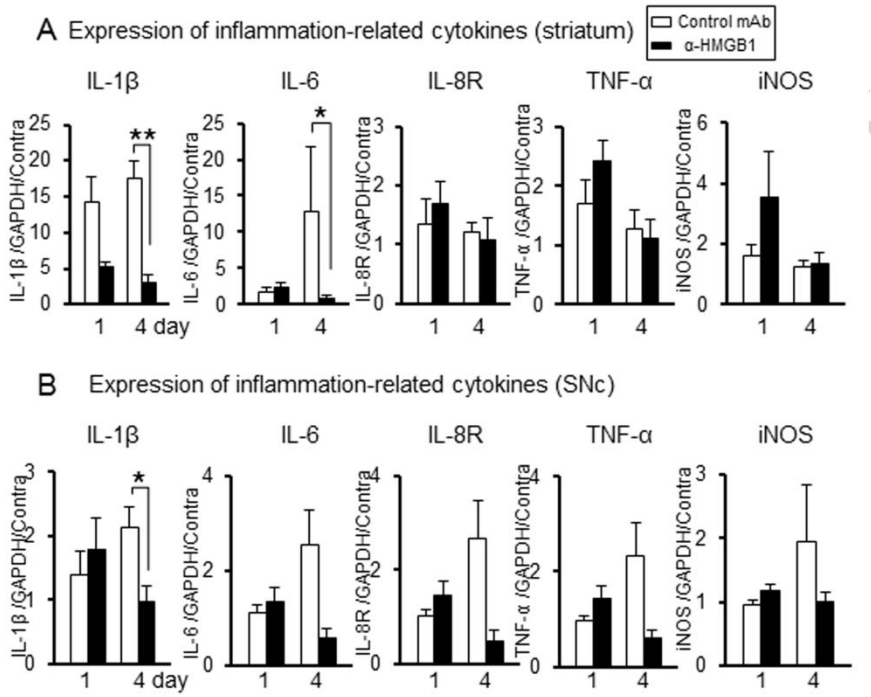

Fig. 8

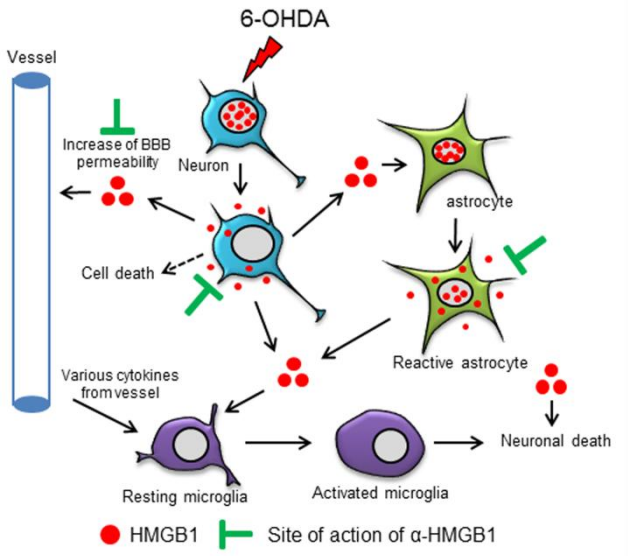

Fig. 9

Highlights

We explore the dynamics of HMGB1 on a rat model of PD.

Anti-HMGB1 Ab exerts neuroprotection for a rat model of PD.

Anti-HMGB1 mAb suppresses inflammatory responses.

Anti-HMGB1 mAb attenuates disruption of BBB induced by 6-OHDA.